

V. GEOPHYSICS

Prof. F. Bitter
 Prof. G. Fiocco
 Dr. T. Fohl
 Dr. W. D. Halverson

Dr. J. F. Waymouth
 R. J. Breeding
 J. C. Chapman
 A. J. Cohen
 J. B. DeWolf

R. J. DiGrazia
 G. W. Grams
 H. C. Koons
 K. Urbanek

A. PLASMA DIFFUSION IN A MAGNETIC FIELD

Experiments on the transverse diffusion of plasma in low-pressure arc discharges have continued since the last report.¹ The discharge tube shown schematically in Fig. V-1 was filled with argon at 0.5 torr pressure and operated in longitudinal magnetic fields up to 1.8 Wb/m^2 . The magnetic field is homogeneous to 1.3 per cent over a 140-cm length of the tube that includes all of the plasma probes.

1. Two-Mode Operation

The occurrence of the two-mode operation found previously¹ is strongly influenced by the alignment of the discharge tube with respect to the magnetic lines of force. For fields approximately $0.25\text{-}0.8 \text{ Wb/m}^2$, the axial electric field E_z can be varied by as much as a factor of 10 by tilting the tube one or two degrees with respect to the magnetic lines. The onset of the high electric field ("turbulent mode") is sudden and is accompanied by increased light and electrical noise output. In this range of magnetic field strength, the discharge is channeled by the converging magnetic lines at the solenoid coil nearest the cathode end of the tube. The visible plasma is concentrated in a column of approximately 2-cm diameter which expands to refill the tube at a distance downstream that is determined by the magnetic field and the degree of turbulence of the discharge. The first center probe (Probe 2 in Fig. V-1) is approximately 25 cm from the center

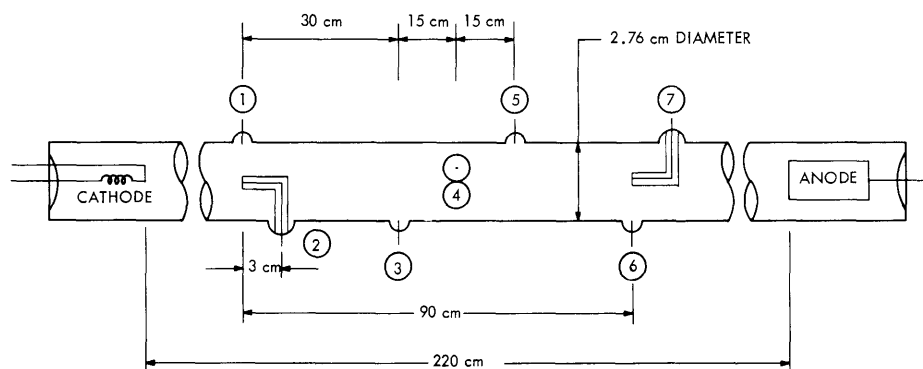


Fig. V-1. Schematic diagram of the discharge tube. All probes made of 40-mil tungsten wire. Center probes encased in 3-mm glass sheaths, cut flush at the end to expose the probe.

(V. GEOPHYSICS)

line of the end coil of the solenoid, and is in a region of high plasma density. The probe causes a plasma perturbation at these magnetic fields which sets up a bright glow around the probe, extending approximately 10 cm on the anode side and 1 cm on the cathode side. A bright beam of plasma, approximately 2 mm in diameter, also extends from the probe for a distance of 20-30 cm toward the cathode.

It is likely that the two-mode operation is associated with the plasma disturbance caused by Probe 2. The turbulence appears to set in just when the compressed discharge column no longer intercepts the probe. The perturbation may tend to smooth out the radial plasma density gradients that, according to Kadomtsev,² are necessary for the onset of spiral instabilities in the discharge column. Further evidence supporting this hypothesis is the fact that the strength of turbulence is a direct function of the discharge current. When the current is increased from 0.5 amp to 0.7 amp, the discharge will no longer remain in the low-voltage mode. The density gradients are almost directly proportional to the discharge current (under the assumption of constant longitudinal electron drift velocity), and it seems likely that the smoothing effect of the probe disturbance is overshadowed by the destabilizing tendency of the increased plasma density gradients.

2. Longitudinal Inhomogeneity

The longitudinal plasma inhomogeneity, observed visually, is also evident from electrical measurements. Figure V-2 shows the axial electric field E_z calculated from the floating potential drop between Probes 6 and 1 compared with E_z from Probes 6 and 5. The radial potential drop V_r , defined as

$$V_r = V_{\text{wall}} - V_{\text{center}},$$

is also shown for measurements at opposite ends of the discharge. The curves indicate that the electron flux to the tube walls is considerably greater at the anode end than at the cathode end when the discharge is in the turbulent state. The fact that the strong departure from longitudinal homogeneity occurs at the onset of turbulence indicates that the turbulence itself is not uniformly distributed over the length of the tube, tending to be more concentrated toward the anode.

As the magnetic field is increased above 1.0 Wb/m^2 , the discharge becomes more longitudinally homogeneous, both visually and from electrical measurements. At this point the visible discharge does not completely fill the tube throughout the length of the solenoid. As the field is increased to 1.75 Wb/m^2 , the discharge becomes somewhat more compressed at the cathode end of the solenoid, and the expansion angle downstream steadily decreases. At maximum magnetic field, the visible discharge is concentrated in a diameter of approximately 1 cm at the cathode end and 2-3 cm at the anode end of the solenoid. The E_z and V_r measurements in different parts of the tube also tend

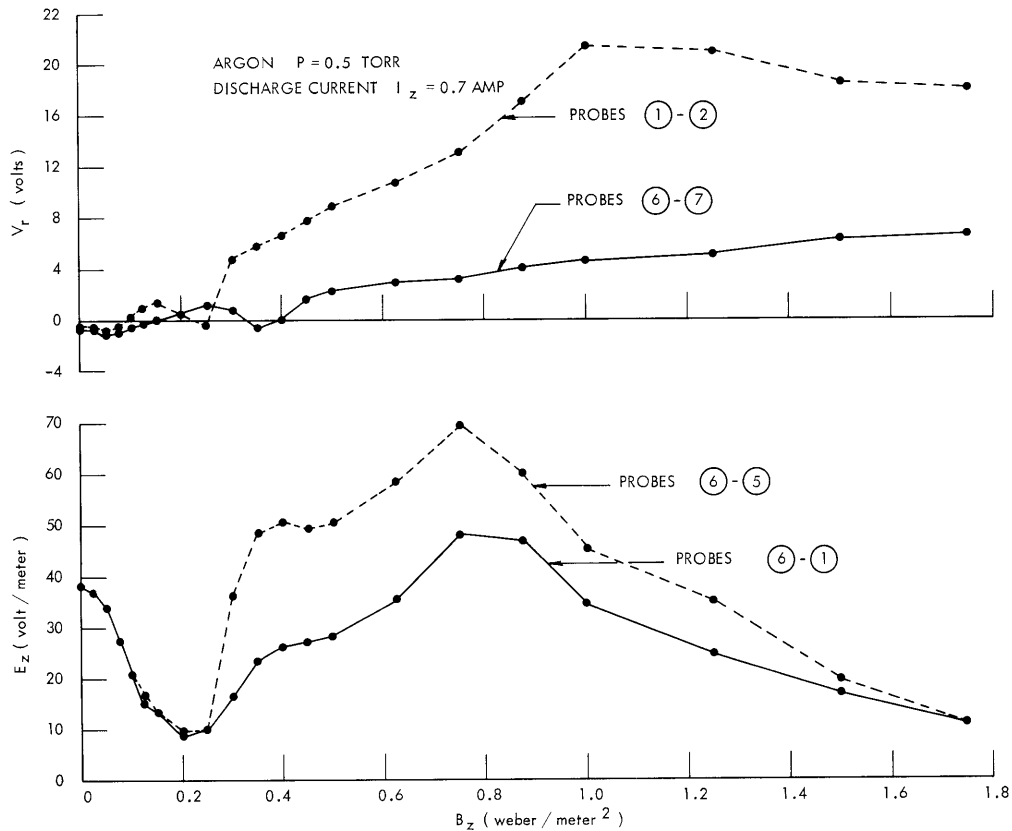


Fig. V-2. Axial electric field and radial potential drop measured by probes indicated in Fig. V-1.

toward uniform values at this magnetic field.

Tests with the anode or cathode in the homogeneous magnetic field region indicate that the axial position of the discharge electrodes does not influence the qualitative behavior of the plasma column in the magnetic field. The results are also independent of the polarity of the solenoid electromagnet.

W. D. Halverson

References

1. W. D. Halverson, "Plasma Diffusion in a Magnetic Field," Quarterly Progress Report No. 75, Research Laboratory of Electronics, M.I.T., October 15, 1964, p. 31.
2. B. B. Kadomtsev, "Convection of the Plasma of a Positive Column in a Magnetic Field," Soviet Phys. - Tech. Phys. 6, 927-933 (1962).

B. RECOMBINATION COEFFICIENT MEASUREMENT BY LANGMUIR PLASMA PROBE

A simple technique is being used for determination of recombination coefficients in noble gases plasmas. A plasma is generated by running a DC discharge at the center

(V. GEOPHYSICS)

of a large glass sphere (radius, 25 cm) filled with noble gas. Radial distribution of electron temperature and density is then measured by means of a movable Langmuir probe. Under the assumptions that the electron temperature is much greater than the ion temperature, ions are positive and singly ionized, and the plasma is neutral, the equation governing the diffusion of ions and electrons radially towards the walls of the glass sphere is

$$\Gamma_r = -\frac{k}{e} \mu_i \frac{d}{dr} [n_e (T_e + T_i)], \quad (1)$$

where

Γ_r = net flow of electrons or ions per unit area perpendicular to r

μ_i = ion mobility

n_e = number density of electrons

T_e, T_i = ion and electron temperatures.

If all of the ions and electrons are produced at the center of the tube (which is also the origin of the coordinate system) and there is no loss of ions or electrons, then the flow Γ_r at a given radius r is

$$\Gamma_r = \frac{Z_i}{4\pi r^2}, \quad (2)$$

where Z_i is the rate of production of ions at the origin. Equating (1) and (2) and integrating, we obtain the expression for $n_e (T_e + T_i)$ as a function of radius r

$$n_e (T_e + T_i) = \frac{eZ_i}{4\pi k \mu_i} \cdot \frac{1}{r} + C. \quad (3)$$

The constant C can be determined from the boundary conditions. In a simple case we neglect the presence of the glass sphere; therefore, we can set $n_e (T_e + T_i)$ as zero at infinity. The constant C is then zero. Plotting the quantity $n_e (T_e + T_i)$ against $1/r$,

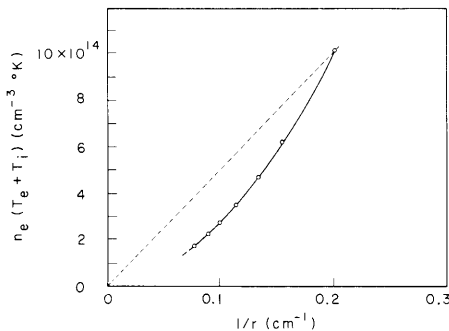


Fig. V-3.

$n_e (T_e + T_i)$ as a function of $1/r$ for Argon plasma. Dotted line represents diffusion without recombination; solid line (actual values) indicates recombination.

we shall obtain a straight line connecting the origin with the value of $n_e(T_e + T_i)$ at the particular radius (dotted line in Fig. V-3). The slope of this line will be

$$\frac{eZ_i}{4\pi k\mu_i}$$

If, however, recombination takes place in the diffusing plasma, Z_i will vary with the radius and we no longer have a straight line. In this case we can interpret the quantity $Z_i = Z_i(r)$ as "apparent" or "net" rate of ion production inside the particular radius, and the slope of the curve will decrease with decreasing $1/r$ (Fig. V-3).

Electron temperature and density at various radii can be measured by means of a movable Langmuir probe. From the measurements, the "apparent" production rates can be determined for different values of r . Calculating the decrease in "apparent" production rate between two radii, we can determine how many ions are lost because of recombination. Dividing this value by the difference of volume of the two corresponding spheres, we obtain the number of recombination events per unit of volume per second, R .

The recombination coefficient α is then defined by the relation

$$R = \alpha n_i n_e. \quad (4)$$

We have determined the recombination coefficient for an Argon plasma with electron density $1 \times 10^{11} \text{ cm}^{-3}$ and temperature $9,000^\circ\text{K}$ as $5 \times 10^{-10} \text{ cm}^3 \text{ sec}^{-1}$.

K. Urbanek

References

1. E. W. McDaniel, Collision Phenomena in Ionized Gases (John Wiley and Sons, Inc., New York, 1964).
2. S. C. Brown, Basic Data of Plasma Physics (The Technology Press of the Massachusetts Institute of Technology, Cambridge, Mass., and John Wiley and Sons, Inc., New York, 1959).

C. PROTON FLOW INTO THE MAGNETOSPHERE

Recent measurements of the proton flow in the transition region and in interplanetary space from the Imp-1 satellite have been reported by Olbert and Moreno,¹ Lyon et al.,² and Egidi et al.³ The data covering the energy range 45-5400 eV give evidence for ordered flow in the transition region.

On the basis of these measurements, we have carried out a simple continuity calculation that may be interpreted as suggesting a transfer of protons between the transition region and the magnetosphere. The geometry is shown in Fig. V-4. The boundaries of the transition region that give the best paraboloidal fit to the position of the observed discontinuities were rotated about the earth-sun line through a small angle, θ , above and

(V. GEOPHYSICS)

below the ecliptic plane. The proton flow per second per degree of latitude, θ , crossing a plane perpendicular to the flow at an hour angle, ϕ , as calculated from the

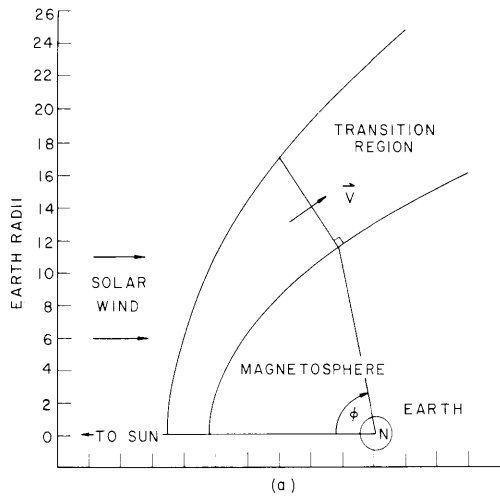
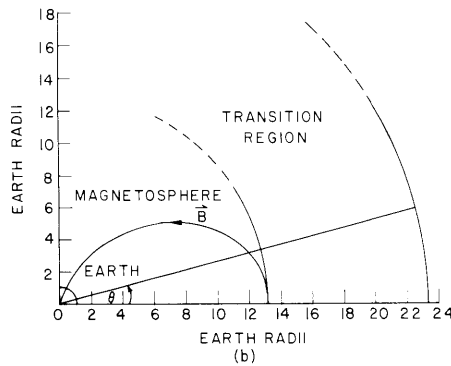


Fig. V-4

- (a) Boundaries of the transition region in the ecliptic plane.
- (b) Dawn meridian cross section showing the transition region and a magnetic field line resulting from a centered dipole.



Imp-1 data, is illustrated in Fig. V-5 (curve a). One point representing almost a three-fold increase in the proton flow in the transition region at $\phi = 85^\circ$ was obtained on February 12, 1964, during a period following a sudden-commencement magnetic storm. Although inserting this point in the data would not contradict the results of this calculation, it has been omitted from curve a. The density and flow velocity are averages across the transition region. Curve b is the flow expected, under the assumption that all particles from the solar wind enter and remain in the transition region and that there is no flow across the inner boundary. The curve is drawn for a solar wind flux of 2×10^8 protons $\text{cm}^{-2} \text{sec}^{-1}$.

The data indicate that the total number of particles crossing a plane at a given hour angle is generally greater than can be accounted for by the solar wind alone.

If we assume that there is no ordered flow of protons in the θ direction in the transition region, we can account for the additional protons by allowing flow between the

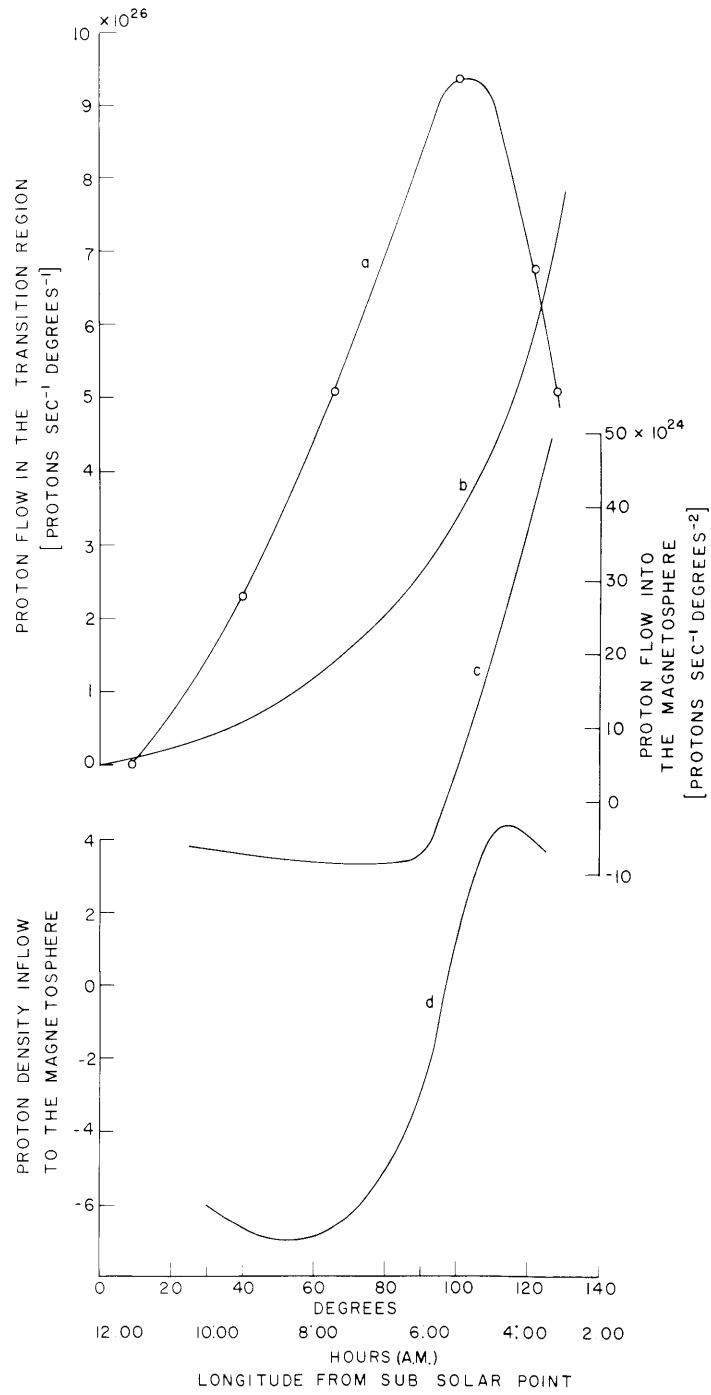


Fig. V-5. (a) Observed proton flow in the transition region (particles per second per degree, θ) crossing a plane perpendicular to the flow at an hour angle, ϕ .
 (b) Expected proton flow in the transition region for a solar wind flux of 2×10^8 protons $\text{cm}^{-2} \text{sec}^{-1}$.
 (c) Protons flowing into the magnetosphere per second per degree, θ , per degree, ϕ , required to account for the measured number of protons in the transition region in excess of those coming directly from the solar wind.
 (d) Curve (c) normalized by $1/r^3$ to represent a flow density.

(V. GEOPHYSICS)

magnetosphere and the transition region. The number of protons flowing into the magnetosphere per second per degree, θ , per degree, ϕ , required to account for the measured number of protons in the transition region in excess of those coming directly from the solar wind is illustrated in curve c. It is found that flow is required from the magnetosphere to the transition region during the hours from 6 a. m. to 10 a. m., and from the transition region to the magnetosphere from 3 a. m. to 6 a. m. There is qualitative agreement between this behavior and the flow patterns in the model of the magnetosphere as postulated by Hines.⁴ It would seem unlikely that recombination could cause the particle loss observed in the transition region before 6 a. m.

If this influx is further normalized by a factor $1/r^3$, where r is the distance from the center of the earth to the inner boundary of the magnetosphere, to take into account the volume of the flux tube exposed to the boundary, it is found that the maximum inflow density occurs around 5 a. m., as shown in curve d. This finding corresponds approximately with the time of peak occurrence of the VLF emission known as chorus (Laaspere, Morgan and Johnson⁵). Several mechanisms have been proposed for the generation of VLF emissions. Two of these involve protons in the magnetosphere. MacArthur⁶ has suggested Doppler-shifted cyclotron radiation from protons, and Kimura⁷ has suggested a transverse resonance plasma instability for a beam of protons.

H. C. Koons, G. Fiocco

References

1. S. Olbert and G. Moreno, "Analysis of the solar wind in the transition region," *Trans. Am. Geophys. Union* 45 (4), 588 (1964).
2. E. Lyon, H. Bridge, A. Egidi, and B. Rossi, "Imp-1 plasma summary data," *Trans. Am. Geophys. Union* 45 (4), 588 (1964).
3. A. Egidi, H. Bridge, E. Lyon, and B. Rossi, "Spatial properties of the interplanetary plasma and its interaction with the Earth's field as observed on Imp-1," *Trans. Am. Geophys. Union* 45 (4), 588 (1964).
4. C. O. Hines, "Hydromagnetic motions in the magnetosphere," *Space Sci. Revs.* 3, 342-379 (1964).
5. T. Laaspere, M. G. Morgan, and W. C. Johnston, "Chorus, Hiss and other audio-frequency emissions at stations of the whistler-east network," *Proc. IEEE* 52, 1331-1349 (1964).
6. J. R. MacArthur, "Theory of the origin of the very-low frequency radio emissions from the earth's exosphere," *Phys. Rev. Letters* 2 (12), 491-492 (1959).
7. I. Kimura, "Amplification of the VLF electromagnetic wave by a proton beam through the exosphere, an origin of the VLF emissions," *Rep. Ionosphere Space Res. Japan*, 15 (2), 171-191 (1961).